Microbiology Spectrum
American Society for Microbiology Press

Role of Shiga/Vero Toxins in Pathogenesis

FUMIKO OBATA[1] and TOM OBRIG[1]
[1]University of Maryland School of Medicine, Baltimore, MD 21201

ABSTRACT Shiga toxin (Stx) is the primary cause of severe host responses including renal and central nervous system disease in Shiga toxin-producing *Escherichia coli* (STEC) infections. The interaction of Stx with different eukaryotic cell types is described. Host responses to Stx and bacterial lipopolysaccharide are compared as related to the features of the STEC-associated hemolytic-uremic syndrome (HUS). Data derived from animal models of HUS and central nervous system disease in vivo and eukaryotic cells in vitro are evaluated in relation to HUS disease of humans.

ACTIVITIES OF Stx AND LPS IN RENAL DISEASE

Shiga Toxin Actions

It is generally accepted that all actions of Shiga toxin (Stx) depend on its interaction with the receptor, globotriaosylceramide (Gb_3), on eukaryotic cells. Although alternative receptors for Stx have been postulated, no definitive data have been forthcoming in support. Stx holotoxin is internalized by receptor-mediated endocytosis, retrograde transported via the Golgi apparatus and processed through in the endoplasmic reticulum, and released into the cytoplasm where it enzymatically inactivates ribosomes and inhibits protein synthesis (Fig. 1). However, it is important to note that, in addition to Stx holotoxin, the B-subunit alone can interact with Gb_3 in a physiologically meaningful manner where it activates signal transduction pathways in target cells (Fig. 1) (1). An additional but unexplained anomaly is the interaction of Stx with eukaryotic cells in a Gb_3-independent manner that leads to induction of cytokines by these cells (2). As shown in Fig. 1, intracellular responses to Stx are diverse, including inhibition of protein synthesis, activation of cellular stress responses, and induction of cytokines and chemokines. It is likely that these different schemes take place in cell-specific activities during Shiga toxin-producing *Escherichia coli* (STEC) infections in humans, culminating in typical hemolytic-uremic syndrome (HUS). As depicted, it is clear that in some cases Stx can result in activation of p38 mitogen-activated protein kinase as well as apoptotic and necrotic cell death (Fig. 1). The topic of HUS renal disease has been reviewed recently (3–5).

Cell Types Responsive to Stx

The high number of Stx-sensitive cell types makes more difficult identification of more important events responsible for HUS. Renal microvascular endothelial cells are generally accepted to be the primary target of Stxs in HUS. Data in support of this concept come from many sources, most notably autopsy kidney pathology samples showing swollen and detached endothelial cells accompanied by thrombi (6). Such human renal microvascular endothelial cells were also shown to be very sensitive to Stx in vitro (7). However, other cells that make up the human renal glomerulus are also sensitive to Stx, including podocytes and mesangial cells (8, 9). In addition, extraglomerular epithelial cell

Received: 1 May 2013, **Accepted:** 29 July 2013,
Published: 20 June 2014
Editors: Vanessa Sperandio, University of Texas Southwestern Medical Center, Dallas, TX, and Carolyn J. Hovde, University of Idaho, Moscow, ID
Citation: Obata F, Obrig T. 2014. Role of Shiga/Vero toxins in pathogenesis. *Microbiol Spectrum* 2(3):EHEC-0005-2013. doi:10.1128/microbiolspec.EHEC-0005-2013.
Correspondence: Fumiko Obata, fobata@som.umaryland.edu

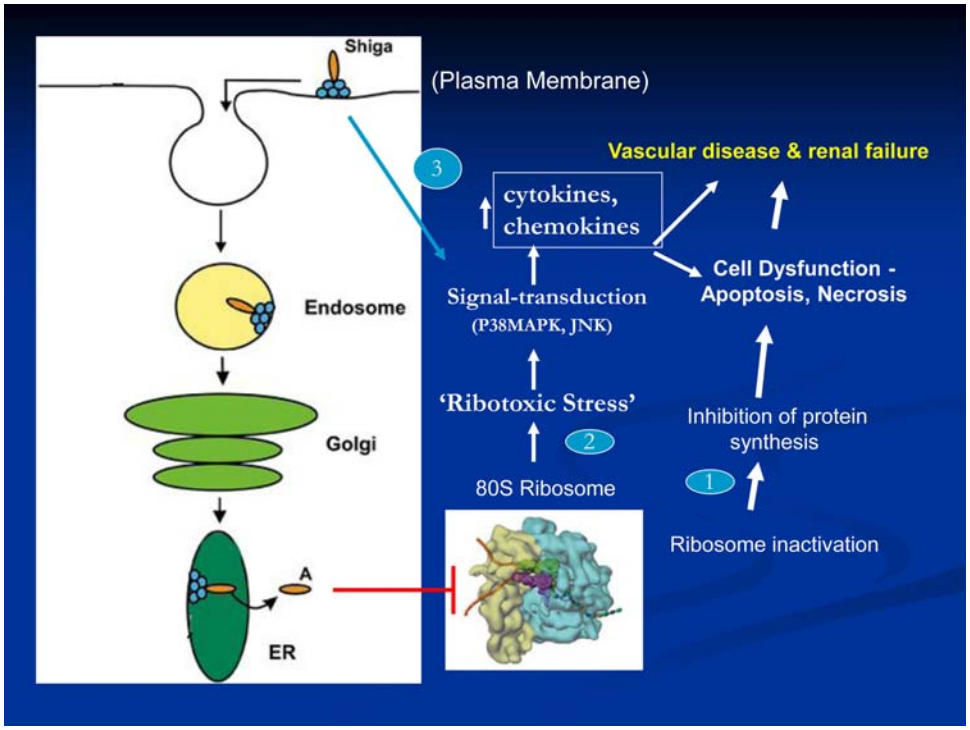

FIGURE 1 Schema: Shiga toxin interaction with eukaryotic cells. doi:10.1128/microbiolspec.EHEC-0005-2013.f1

types of the human kidney have been postulated to be targets of Stx, including proximal tubule and collecting duct cells (8, 10, 11). Cell types in the blood circulation that may be key to development of HUS and that are sensitive to Stx include platelets, neutrophils, and monocytes (12–16).

In summary, most, if not all, of the cell types mentioned may well have a role in STEC-related kidney disease and typical HUS. The relative importance and role of these cell types in STEC HUS remain to be determined. For example, it is not clear which of the renal cell types are actually responsible for renal failure in STEC HUS, although apoptosis of tubules appears to be a common feature (8, 17). The relative contributions in HUS disease of renal microvascular coagulation and thrombosis (i.e., endothelial cells), imbalance of fluid and electrolytes (i.e., nephron tubules), and altered filtration barrier function (i.e., endothelial and podocyte cells) have yet to be elucidated for typical HUS. If in vitro cell culture studies are pertinent to HUS in patients, the sensitivity (50% lethal dose) of human renal cells to Stx2 (endothelial, 0.1 pM > podocyte, 0.5 pM >> proximal tubule, 10 pM) suggests the renal filtration barrier is at considerable risk (8).

Inflammatory Cells, Chemokines, and Renal Thrombosis

A primary feature in the renal pathology of STEC HUS is microvascular coagulation and thrombosis. In humans and in a murine model of HUS, the interaction of Stx and lipopolysaccharide (LPS) with circulating cells and resident renal cells appears to have a causal role in microvascular thrombosis (18, 19). In a series of studies of the Stx/LPS murine model of HUS, a pathway leading to fibrin deposition was revealed (Fig. 2). LPS activation of cells such as endothelial and renal tubule cells elicited chemokines (monocyte chemotactic protein 1 [MCP-1], macrophage inflammatory protein 1 [MIP-1] alpha, RANTES) known as chemoattractants for monocyte/macrophage cells and coactivators of platelets. In this response, Stx enhances the effects of but does not replace LPS. The response was associated with renal fibrin deposition (12, 20). In the murine model, simultaneous neutralization of these three chemokines inhibited LPS/Stx-induced monocyte accumulation and fibrin deposition in the kidneys (20). Further, administration of adenosine A2a receptor agonists to Stx/LPS mice also reduced monocyte and fibrin accumulation in the kidneys. As shown in Fig. 3, adenosine A2a receptor agonists act as anti-inflammatory agents in monocytes,

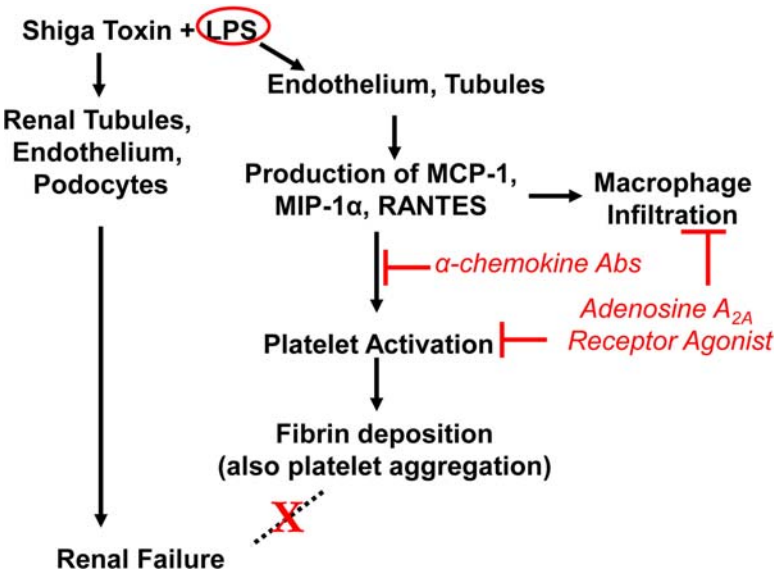

FIGURE 2 Proposed pathways of Stx and LPS actions in mice. Data derived from a Stx/LPS murine model of HUS indicate that LPS is the primary elicitor of fibrin deposition in kidneys. This pathway requires chemokines and platelets but is not responsible for renal failure. Stx is responsible for renal failure in this murine model in a process that involves nonendothelial renal cell types. doi:10.1128/microbiolspec.EHEC-0005-2013.f2

platelets, and endothelial cells (21). Taken together, these studies indicate that both LPS and Stx are required for maximal renal fibrin deposition and that platelets may be required. Because mice deficient in MCP-1 have sharply reduced platelet deposition after exposure to Stx/LPS, we have suggested that this chemokine serves as a coactivator of platelets in typical HUS (Keepers TR, unpublished data). The primary activators of platelet activation are thrombin or adenosine diphosphate. Our renal gene array analysis of the LPS response in mice indicated that LPS strongly elicited fibrinogen mRNA, the precursor of fibrin (Obrig T, unpublished data). In addition, it is noteworthy that selective elimination of monocytes from mice prior to the above studies had no effect on the ability of Stx/LPS to elicit renal fibrin deposition, suggesting the chemokines are being generated from other cell types such as renal tubules (20). Important conclusions from the murine HUS model are that LPS, not Stx, is the initial primary elicitor of renal coagulation and thrombosis, but Stx, not LPS, is the lethal agent of STEC.

In the murine Stx/LPS model of HUS, monocyte migration into the kidneys was restricted to the extraglomerular space in contrast to polymorphonuclear leukocytes (PMN), which, in addition, migrated into the glomeruli. The latter may be important in humans because neutrophilia has been implicated as a primary risk factor for HUS disease and increased neutrophil migration into the kidneys was a key observation in HUS renal biopsies (22, 23). In the murine model of HUS, the neutrophil chemotactic factors chemokine ligand 1 (CXCL1) keratinocyte-derived chemokine (KC) and CXCL2 (MIP-2) were induced in the kidneys by LPS (15). The induction was at the transcriptional level and was enhanced by Stx2. Administration of neutralizing antibodies for these neutrophil chemotactic factors prevented the movement of neutrophils into the kidneys. It was also demonstrated that vascular cell adhesion molecule 1 (VCAM-1) was induced in the kidneys simultaneously with CXCL-1 and CXCL-2 in response to Stx2/LPS in mice (Fig. 4). VCAM-1 is known to assist movement of neutrophils across the endothelium and appeared to exhibit this function for neutrophils in the Stx2/LPS murine model of HUS. However, the relative importance of renal neutrophils in Stx-induced renal failure has yet to be determined in mice and humans.

Renal Gene Array Analysis of Murine Responses to Stx2 and LPS

Much information is now available regarding the biological effects of Stx2 and LPS on kidneys in the murine HUS model. The following is a synopsis of the more pertinent gene microarray data obtained from temporal studies of the murine renal responses to Stx2, LPS, or Stx2/LPS (19). On the basis of the total of both up- and downregulated genes, five times more renal genes responded to LPS than to Stx2 over the 72-h time course. Response to LPS was mostly early, whereas Stx2 responses occurred later in the 72-h time course. These results are more meaningful when viewed in the larger picture of HUS where renal failure occurs later in the time course in both mice and humans. It should be emphasized that Stx2, rather than LPS, is the lethal factor in the murine HUS model. The gene array data revealed

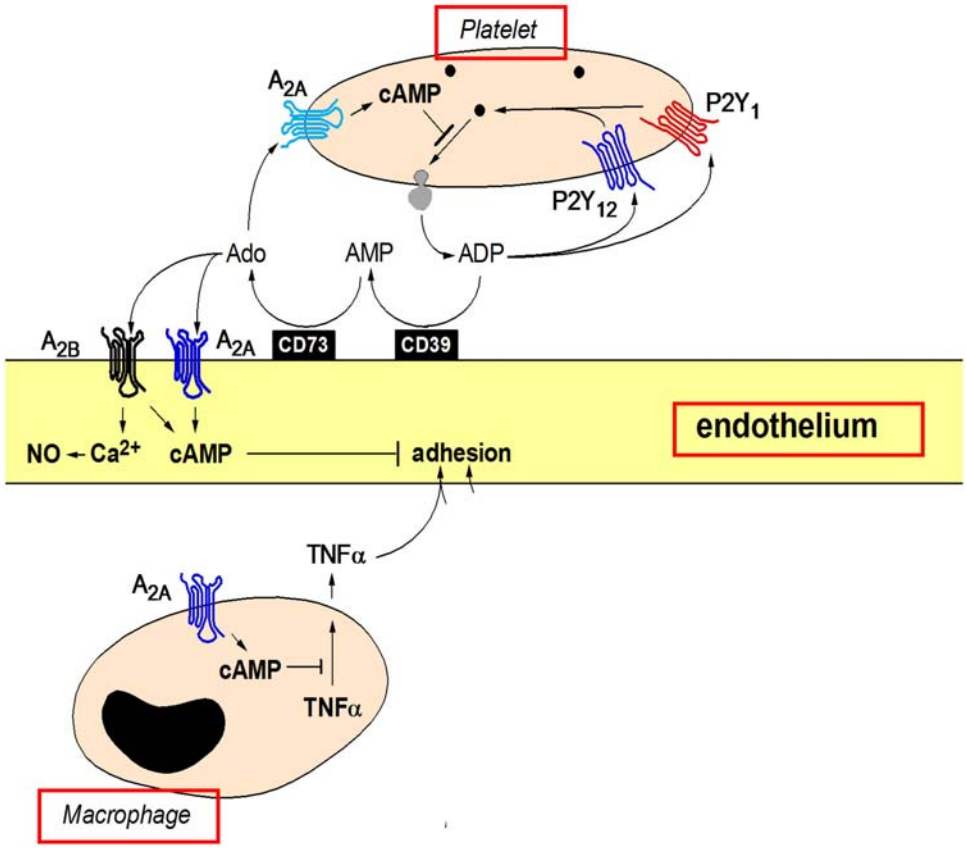

FIGURE 3 Anti-inflammatory actions of adenosine in HUS. Data derived from an Stx/LPS murine model of HUS suggest adenosine A2a receptor agonist, i.e., adenosine, effectively blocks the actions of LPS (enhanced by Stx2) at the level of different renal cell types to prevent platelet activation and coagulation. doi:10.1128/microbiolspec.EHEC-0005-2013.f3

different roles for LPS and Stx2 in the renal physiological responses. LPS responses were mostly inflammatory, stress related, or cell defensive in nature. In contrast, Stx2 responses were related to cell repair and involved cell proliferation and differentiation or cell cycle control genes. An interesting finding was that renal genes down-regulated by Stx2 included membrane transporters, which appeared to signal a protective survival mode and slowing of cell metabolism.

The renal genes most upregulated by Stx2 or LPS are depicted in Fig. 5. As expected from the inflammatory responses described above, LPS induced a number of chemokine genes that code for chemotactic factors for monocytes and neutrophils. These tend to be "immediate" response genes, which attract monocytes and neutrophils into the kidneys and set the stage for a broad inflammatory response in the kidneys. Such LPS "immediate" response genes are mentioned in the literature in descriptions of typical HUS, i.e., MCP-1, MIP-2alpha, and the murine interleukin-8 mimic, KC. It was also observed that interferon-gamma-inducible protein-10 (IP-10) (CXCL10) was induced by LPS and by Stx2, albeit in early and late parts of the HUS disease time course, respectively. Related to renal coagulation and thrombosis in HUS, LPS induced a set of fibrinogen genes "late" in the time course of the murine model of HUS concomitant with the appearance of fibrin deposition and coagulation in the renal microvasculature of HUS (Fig. 5). These data agree with our observation that LPS is responsible, in part, for fibrin deposition in the Stx2/LPS murine model of HUS (19). Amyloid protein, which has been reported to be a Stx-sensitizing factor in HUS, is induced at the mRNA level by LPS in mice, as shown in Fig. 5, as a renal "late" gene product (24). More recently, complement has been identified as a factor that may contribute to renal failure in atypical HUS.

Products of some of the genes shown in Fig. 5 have been examined by investigators as potential biomarkers for diagnostic purposes. For example, IP-10 has been identified as a urine biomarker for other kidney diseases such as lupus nephritis (25, 26). Lipocalin 2 (neutrophil gelatinase-associated lipocalin), an LPS-induced "early"

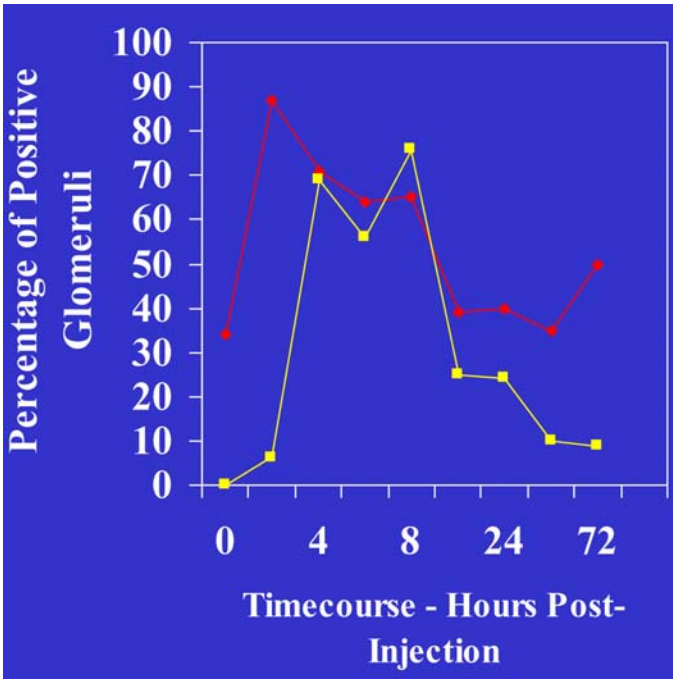

FIGURE 4 Neutrophil-endothelial cell interactions in HUS. In the Stx2/LPS murine model of HUS, analysis of renal gene activation and neutrophil infiltration into kidneys demonstrates a concomitant increase in PMNs and VCAM-1 expression, suggesting a mechanism of PMN-endothelial association. ◆, Neutrophils in the glomeruli; ■, VCAM-1 in the glomeruli. doi:10.1128/microbiolspec.EHEC-0005-2013.f4

gene (Fig. 5), is a common urine biomarker for numerous renal diseases, including STEC-HUS (27).

How Valid Is the Murine Model of HUS for Translation to the Human Disease?

A large volume of data exists for mouse models of Stx-HUS (28). The two common experimental approaches for these murine models are either oral infection with STEC or injection with purified Stx plus or minus LPS (17, 19, 29, 30). In virtually all cases these are lethality models within 4 to 12 days after exposure to the agents and are accompanied by renal damage. Where examined, these murine models usually exhibit the three hallmarks of HUS: thrombocytopenia, hemolytic anemia, and renal failure. However, every animal model has its limitations, and for the murine models of HUS, the renal microvascular endothelial cells do not express Gb_3 and are resistant to Stx action. This is important if one believes that the primary target of Stx is the renal microvascular endothelium. Indeed, human renal endothelial cells in vitro are very sensitive to Stx, and the pathology of human kidneys in HUS describes swollen and detached glomerular endothelial cells. But it is surprising why such human glomerular endothelium is not killed by Stx in HUS kidneys. This suggests either a more indirect action of Stx in human HUS or dominant survival activities are activated within the endothelium after exposure to Stx. An alternative explanation is that the primary target of Stx in human kidneys is not the endothelium, but rather glomerular podocytes and extraglomerular tubules along the nephron. Support for this exists for HUS in mice and humans where urine specific gravity changes, chemokines are increased in the urine, and biomarkers of damaged podocytes and tubule cells are detected.

Mouse models have been helpful in separating the actions of Stx and LPS in HUS. In general, and as described above, LPS is the primary inducer of cytokines and chemokines where Stx enhances the activity of LPS. The complexity of inflammation in HUS is critical but has yet to be fully delineated in murine models and in human HUS. The murine model mirrors typical HUS of humans as resting platelets are resistant to Stx and require preactivation with LPS (19). However, it is most important to reiterate that Stx, not LPS, is responsible for the renal failure in typical HUS. In conclusion, the murine responses to Stx and LPS include most of the features of STEC-HUS in humans.

ACTIVITIES OF Stx IN CNS DISEASE

CNS Symptoms of Animal Models

In either an oral inoculation of STEC model or purified Stx injection animal model, the most common and most frequently reported central nervous system (CNS) impairment is paralysis of extremities. Most frequently, the hind legs are affected first, followed by the forelegs. Other symptoms include anorexia, lethargy, ataxic gait, recumbency (the affected animals lose strength to hold their body in an upright position), convulsions, seizure, coma, and death.

STEC oral administration animal models are summarized in Table 1. The oral inoculation models of STEC that describe CNS symptoms are limited to pig and mouse. Pigs develop "edema disease" with Stx2e-producing *E. coli* and present CNS symptoms (Table 2). Experimentally, the edema disease-like state is reproducible with Stx2-producing *E. coli* that has been isolated from human patients. CNS symptoms are only seen in Stx2 (both Stx2 and Stx2e) producers, but not in non-Stx2 producers. This indicates a strong association of Stx2 with CNS impairment.

LPS is an outer membrane component of gram-negative bacteria and a strong inflammation inducer. The involvement of LPS in STEC-associated CNS

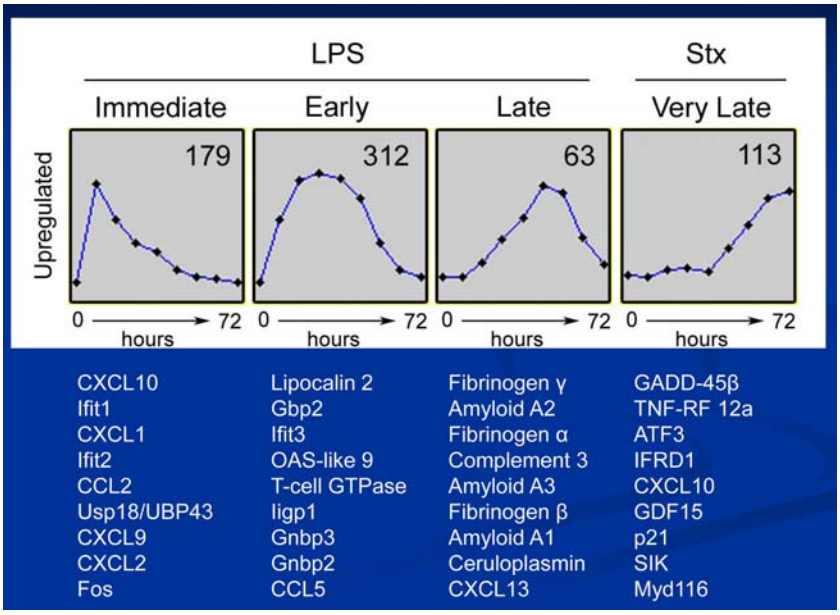

FIGURE 5 Renal gene activation in the Stx/LPS murine model. Shown are the nine most upregulated genes in the temporal response of mice to either LPS or Stx2. Gene microarrays were employed to analyze kidney gene activation over a 72-h response of C57BL/6 mice to 300 μg/kg of LPS or 100 ng/kg of Stx2. doi:10.1128/microbiolspec.EHEC-0005-2013.f5

symptoms was tested by using LPS nonresponder mouse C3H/HeJ (29). C3H/HeJ did present CNS symptoms when given Stx2-producing *E. coli* but not when Stx-nonproducer was inoculated. This again suggests a strong involvement of Stx in CNS symptoms. The difference between LPS-responder mouse (C3H/HeN) and C3H/HeJ in CNS symptoms was that C3H/HeN showed a progressive time course of CNS symptoms whereas C3H/HeJ showed a "biphasic" response in that they developed milder CNS symptoms and recovered once, but then progressed to a severe form of CNS impairment. This suggests that even though Stx2 may be the central cause of CNS symptoms, addition of LPS response may contribute to the progress of the disease.

To further study the action of Stx2 in CNS disease, different animals were tested with purified Stx2. Stx2 injection animal models with CNS complications are summarized in Table 3. Also, LPS involvement or contribution to Stx2-associated CNS disease was tested in some reports. The reproducible results of hind-leg paralysis and high frequency of convulsions and seizures with purified Stx confirm the central role of the toxin in STEC-associated CNS disease. Human STEC patients present CNS symptoms that range from eye involvement (diplopia, hallucinations, and cortical blindness), behavioral changes (hyperactivity, distractibility, irritability, and altered sensorium), posturing/coordination difficulties (poor fine-motor coordination, hemiplegia, ataxia, and clumsiness), to severe symptoms such as seizures, dysregulation of breathing, and alteration in consciousness such as coma. Within these varieties of symptoms, ataxia or hemiparesis resembles Stx-associated animal CNS symptoms. Also, it is notable that in human patients, seizures are a frequent observation. This resemblance between patients and animal models of STEC/Stx suggests there is a great possibility that analyzing these animal models may give some clues to define the mechanisms of CNS impairment in Stx-associated disease.

CNS Histopathology of Animal Models

In animal models with STEC oral inoculation that describe CNS symptoms, most exhibit defective capillaries (pig [31–34], mouse [35, 36]). Those capillary lesions are mostly related to endothelial cell weakening that appears as hemorrhage, with leaked red blood cells in parenchyma. Noncapillary components in the parenchyma such as neurons and myelin defects were seen in some mouse STEC models (35, 37, 38), but not others (36). In purified Stx2 injection models, similar lesions involving capillary/endothelial cells were found in pig (39, 40), rabbit (41–43), and mouse (44, 45). In contrast, other models did not have these lesions but rather lesions related to neuronal degeneration (baboon [46], rabbit [43, 47, 48], rat [49, 50], mouse [51]) or myelin degeneration (baboon [46], rabbit [52], rat [49]). Also, some reports showed normal appearance of neurons (rabbit [47], striatal neurons; mouse [53] lumbar spinal cord neurons). As all models exhibit similar CNS symptoms such as hind-leg paralysis, the difference in histopathological lesions may be due to involvement of different parts of CNS, different time points in the disease, or species-specific sensitivities. The mechanism of inducing CNS symptoms may be weakening of endothelial cells/capillary composition-caused neurotoxicity or direct

TABLE 1 STEC oral administration model with CNS descriptions

Ref.	Animal	*E. coli* strain	CNS[a]	Histopathology[b,c,d]	IHC[e]/TUNEL[b,c,f]	Model notes	Other assays
31	Pig	RCH/86 (Stx2+)	Yes	HE: CL cap, small inf, small hrrg, fib in sub and cap	ND	Gnotobiotic (cesarean section derived)	NA
32	Pig	86-24 (Stx2+)	Yes	Gross: MO and CL hrrg and necPAS: MO, CL, and Sc, cap swl nec, peri deposits	ND	Suckling (colostrum provided)	NA
32	Pig	87-23 Stx (–)	No	No lesion	ND	Suckling (colostrum provided)	NA
33	Pig	S1191 (Stx2e+) M112 (Stx2e+)	Yes	EM: myo and cap nec not apop, mono apop	TUNEL + myo in MO (5/11 pigs)	3-w-o	NA
33	Pig	Strain 123 (non-pathogenic *E. coli*)	No	No lesion	ND	3-w-o	NA
34	Pig	sakai	Yes	LFB: mye deg, hrrg, pyk and prolif cap, peri ede	ND	Neonatal	NA
35	ICR mouse	E32511/HSC (Stx2c+)[i]	ND	EM: cap ede in CR ctx, mye degHE: hrrg and ede in CR ctx only in CNS symptom (+) mice	Immuno EM-DAB[g]: Stx2+ in CR ctx pyr and deg mye	Sm, MMC[h]	Tracer (i.v.) detected in cap and deg mye
29	C3H/HeN mouse	86-24, 86BL or 134 (Stx2+)	Yes	ND	ND	Fasted	NA
29	C3H/HeN mouse	87-23, 87BL (Stx2–)	Yes	ND	ND	Fasted	NA
29	C3H/HeJ mouse	86-24, 86BL or 134 (Stx2+)	Yes (biphasic)	ND	ND	Fasted	NA
29	C3H/HeJ mouse	87-23, 87BL (Stx2–)	No	ND	ND	Fasted	NA
36	C57BL/6 mouse	N-9 (Stx1+/Stx2+)	ND	HE: infilt, hrrg, cap with fib in CR ctxLFB: No deg mye in hippo	Anti-Stx + hippo	PCM[j]	NA
37	IQI mouse	EDL931 (Stx1+/Stx2+)	Yes	HE: ede, fib in cap, neu deg, cap prolif	ND	Gnotobiotic	Brain TNFα increased
55	C57BL/6 mouse	Smr N-9 (Stx1+/Stx2+)	ND	ND	TUNEL + hippo neu during CNS symptom (+)	PCM	Serum Stx ↑, TNFα ↑, IL10 ↑TLC-anti-PkMab[k] brain +
38	IQI mouse	O157:H7 strain 6 (Stx1+/Stx2+)	Yes	HE: CR ctx and CL neu nec and slight loss of Purkinje	ND	Gnotobiotic	ND
56	ICR mouse	E32511/HSC (Stx2c+)	Yes	ND	GFAP[m] ↑, AQP4↓, casp3↑[n]neu cer Sc ventral and MO dorsal	Sm, MMC	ISH[l] Gb3 synthase

[a]Detailed CNS symptoms are summarized in Table 2.

[b]Histopathology analysis keys are Gross, gross observation in nonstained tissue; HE, hematoxylin-esosin stain that stains cytoplasm in pink and nucleus blue, light microscopic findings (LM); PAS, periodic acid-Schiff stain that detects polysaccharides, glycoproteins, and glycolipid, LM; LFB, Luxol fast blue stain that stains myelin in blue, LM; EM, electron microscopic findings; ND, not described; NA, not applicable.

[c]CNS regions and cell type abbreviations are CR, cerebrum; ctx, cortex; hippo, hippocampus; str, striatum; CL, cerebellum; MO, medulla oblongata; Sc, spinal cord; cer cervical; tho, thoracic; lum, lumbaris; sub, subarachinoid space; BS, brain stem is used where midbrain, pons, or medulla oblongata is not specified. Histopathologic feature abbreviations are cap, endothelial cells or capillaries; inf, infarction; hrrg, hemorrhage; fib, fibrin deposition; nec, necrosis; swl, swelling; peri, perivascular; myo, myocytes; apop, apoptotic; mono, monocytes; mye, myelin; deg, degeneration; pyk, pyknotic nuclei; prolif, proliferation/hyperplasia; ede, edema; pyr, pyramidal neuron; inflt, infiltration of blood cells to parenchyma; neu, neuron; Purkinje, Purkinje cells are large neurons in CL.

[d]Histopathologic feature abbreviations are cap, endothelial cells or capillaries; inf, infarction; hrrg, hemorrhage; fib, fibrin deposition; nec, necrosis; swl, swelling; peri, perivascular; myo, myocytes; apop, apoptotic; mono, monocytes; mye, myelin; deg, degeneration; pyk, pyknotic nuclei; prolif, proliferation/hyperplasia; ede, edema; pyr, pyramidal neuron; inflt, infiltration of blood cells to parenchyma; neu, neuron; Purkinje, Purkinje cells are large neurons in CL.

[e]IHC, immunohistochemistry, immunodetection of the target in the tissue sections.

[f]TUNEL, terminal deoxynucleotidyl transferase dUTP nick end labeling detects DNA fragmentation that is a hallmark of apoptosis.

[g]Immuno-EM-DAB, immunodetection of the target with 3,3′-diaminobenzidine deposition by electron microscopy.

[h]Sm, streptomycin; MMC, mitomycin C.

[i]Sm^r, MMC^r.

[j]PCM, protein calorie malnutrition.

[k]TLC-anti-PkMab (thin layer chromatography with anti-Pk monoclonal antibody detectin).

[l]ISH, in situ hybridization.

[m]GFAP, glial fibrillary acidic protein, an astrocyte marker; an increase of GFAP suggests astrogliosis.

[n]IHC for activated (cleaved) caspase-3.

effect of Stx in neuronal toxicity. The observation of lamellipodia-like processes of glial origin interrupting synaptic connections at the lumbar spinal cord interneuron to motor neuron may explain the resulting hind leg paralysis (mouse [53]). A similar observation is reported in a rat model of striatum neurons (51).

CNS Molecular Physiology of Animal Model

Molecular marker analysis in STEC or Stx animal models suggests possible mechanisms for Stx-associated CNS impairment.

The apoptotic nature of Stx-associated lesions has been described. Terminal deoxynucleotidyltransferase-mediated dUTP-biotin nick end labeling (TUNEL) stain detects fragmented DNA and therefore is often used as an apoptotic assay. Capillaries (pig [33], rabbit [43, 54]), neurons (mouse [55], rabbit [43]), and glial cells (rabbit [43]) have been detected as TUNEL positive. Activated caspase-3 targeted immunohistochemistry has been used for another marker of apoptotic cells. Neurons (mouse [56]) and capillaries (rabbit [54]) have been detected positive. Another pro-apoptotic marker, bax, was found increased in rat neurons (57). Along with electron microscopy observation (rat [49]), some neurons and capillary cells (endothelial cells and pericytes) undergo apoptosis, but some appear as necrotic (rabbit [33]). Careful and detailed information of which area of the CNS and what types of cells in that area present apoptotic features may help elucidate these conflicting results.

Aquaporin 4 (AQP4) is mostly expressed in astrocyte foot processes that have a direct contact with capillaries in the CNS. The reduction of AQP4 suggests that there is alteration in astrocytic foot process, which is important to strengthen the blood-brain barrier (BBB). AQP4 expression decreased in Stx2-injected rat (50) and STEC-infected mouse (56), while astrocytic activation marker glial fibrillary acidic protein increased. This suggests Stx-associated astrocyte activation may participate in weakening the BBB.

An increase in tumor necrosis factor alpha in STEC-inoculated mouse (37) and Stx2-injected rabbit (43) brain along with serum tumor necrosis factor alpha increase in STEC-inoculated rabbit (55) suggests Stx-associated inflammation in the CNS.

Ca^{2+} imaging and electrophysiological study are useful tools to assess direct physiological action of Stx in fresh brain slices. Our group showed Stx2-associated neuronal glutamate release in mouse brain slice (cerebral cortex) indirectly by recording intracellular Ca^{2+} in astrocyte (53). Recently, it is shown that Stx2 induces depolarization of neurons in the thalamic area of female rat (58).

Receptor Gb_3 Expression in Animal Central and Peripheral Nervous Systems (CNS, PNS)

Shiga toxin receptor localization in the animal nervous system has been described for different species. There are three ways to localize Shiga toxin receptor. First is to perform anti-Stx immunodetection in tissues of STEC-infected or Stx-injected animals (rabbit [42, 47, 52], rat [49, 59], mouse [35, 36]). Second is to incubate a naïve tissue section with Stx followed by anti-Stx immunodetection (pig [60]). Third is to recognize Gb_3 as an Stx receptor with anti-Gb_3 immunodetection in tissues. Detecting anti-Gb_3 immunoreaction in the naïve tissue provides a basal expression level and cell types that would be influenced by Stx initially in the course of disease. These include neurons in the mouse spinal cord (53) and other regions of CNS (61). In the Stx-administered tissue, it may or may not indicate the spontaneous Stx receptor expression but certainly indicates cell types responsive to Stx. The cell types that are positive in either of the analyses above often include small vessel endothelial cells (rabbit [42, 43, 47, 52, 62, 63], mouse [45, 64]), neurons (rat [49, 57, 59], mouse [35, 45, 53, 61]), and glial cells (rat [49, 57, 59], mouse [45, 61]). Miyatake and colleagues compared the peripheral nervous system (dorsal root ganglion) of different species with the same method and found that human and rabbit expressed Stx receptor in endothelial cells and neurons, whereas rat and mouse expression was restricted to neurons (62, 63). Our group reported that throughout the mouse CNS, the only nonneuronal cell type to exhibit anti-Gb_3 immunoreactivity was the third ventricle ependymal cell (61). Studies have suggested, in the naïve state, humans and rabbits express Stx receptor in their vessels as well as neurons, and rodents appear to express Gb_3 mainly in neurons. However, it was shown that Stx receptors in the rat CNS are induced by Stx administration (57). Among different species, the receptor expression patterns in different regions of CNS, the cell types, and the amount expressed may be different, but all models present with common CNS impairment such as hind-leg paralysis. This may be interpreted as expression of Stx receptor in endothelial cells is not necessary for toxin to be able to internalize into the CNS parenchyma to have an effect.

In 2006, Okuda et al. (64) reported a 4galt knockout mouse that lacks Gb_3 synthase (alpha 1,4-galactosyltransferase) and therefore produces no Gb_3. In this mouse, originally Gb_3-positive vessels lost their anti-Gb_3 immunoreactivity and became Stx resistant. Gb_3 synthase probe has been applied for an in situ hybridization in the mouse (56) and rat (58) CNS. While metabolic

TABLE 2 Observed CNS symptoms in animal models[a]

Ref.	Animal	Model	ANOX	LTHG	HL para	FL para	ATX	RCM[b]	CV/TR	SZR	Coma	Death	Other
46	Baboon	Stx1	ND[c]	ND	ND	ND	ND	ND	ND	ND	ND	Yes	
67	Baboon	Stx1	Yes	ND	ND	ND	ND	ND	ND	3/6 (50%)	Yes	Yes	
31	Pig	STEC	Yes	Yes	Yes	ND	Yes	Yes	Yes	Yes	Yes	Yes	
71	Pig	STEC	ND	ND	ND	ND	Yes	Yes	ND	ND	ND	Yes	Diarrhea, then CNS+
32	Pig	STEC	ND	ND	Yes	Yes	ND	Yes	Yes	ND	ND	Yes	Paddling
39	Pig	Stx2e i.v.	Yes	ND	ND	ND	Yes	ND	Yes	ND	Yes	Yes	Paddling, extensor rigidity, dyspnea
40	Pig	Sup Stx2e i.v.	ND	ND	ND	ND	Yes	Yes	Yes	ND	Yes	Yes	Paddling, extensor rigidity
33	Pig	STEC	ND	ND	ND	ND	Yes (1/11)	Yes (1/11)	ND	ND	ND	ND	
41	Rabbit	Stx1	Yes	Yes	Yes	ND	Yes	ND	ND	ND	ND	Yes	
42	Rabbit	Stx1 i.v.	Yes	Yes	Yes	Yes	ND	Yes	No	ND	ND	Yes	Ruffled fur, rapid respiration
52	Rabbit	Stx2 i.v.	ND	ND	Yes (50%)	Yes (50%)	Yes (33%)	ND	Yes (50%)	ND	ND	Yes (50%)	Opisthotonic posture
47	Rabbit	Stx2 i.v. and i.t.	Yes	Yes	Yes	Yes	ND	Yes	ND	ND	ND	Yes	
68	Rabbit	Stx2 i.v.	Yes	ND	Yes	Yes	ND	ND	ND	ND	ND	Yes	
54	Rabbit	Stx2 i.v.	Yes	ND	Yes	Yes	ND	ND	ND	ND	ND	Yes	Dyspnea
43	Rabbit	Stx2 i.v.	Yes	ND	Yes (83.3%)	ND	Yes (83.3%)	ND	ND	ND	ND	Yes	
48	Rabbit	Stx2 i.v.	ND	ND	Yes (25%)	ND	ND	ND	Yes (25%)	ND	ND	ND	
57	Rat	Stx2 i.c.v.	ND	Yes	Yes	ND	ND	ND	ND	Yes	ND	Yes	Crawling
35	Mouse	STEC	ND	Yes	Yes	Yes	ND	ND	ND	ND	ND	Death	Deformity of backbone, loss of pain
29	Mouse	STEC	ND	ND	Yes	Yes	Yes	ND	Yes	ND	Yes	Yes	Jerky rhythmic motion
36	Mouse	STEC	Yes	Yes	Yes	ND	ND	ND	(Yes)[d]	ND	ND	Yes	Ruffled fur, jerky rhythmic motion
37	Mouse	STEC	Yes	Yes	Yes	ND	ND	ND	ND	ND	ND	Yes	
44	Mouse	Stx2 i.v.	ND	ND	Yes	ND	ND	ND	ND	ND	ND	Yes	
44	Mouse	Stx2 +LPS i.v.	ND	ND	ND	ND	ND	ND	Yes	Yes	ND	Yes	
38	Mouse	STEC	Yes	Yes	Yes	ND	ND	ND	Yes	ND	ND	Yes	Ruffled fur
53	Mouse	Stx2 i.p.	ND	Yes	Yes	ND	Yes	ND	Yes	Yes	ND	Yes	Retain sense (pain)
56	Mouse	STEC	ND	ND	Yes	ND	ND	ND	Yes	ND	ND	Yes	Spinal deformity

[a]Abbreviations for CNS symptoms are ANOX, anorexia; LTHG, lethargy; HL para, hind-leg paralysis; FL para, foreleg paralysis; ATX, ataxic gait; RCM, recumbency, difficulty holding body upright by itself; CV/TR, convulsions/tremors; SZR, seizure. Injection route abbreviations: i.c.v., intracerebroventricular; i.p., intraperitoneal; i.t., intrathecal; i.v., intravenous.

[b]Lateral, sternal, or dorsal recumbency; the animal is lying down with leaning on its side, abdomen, or back, having difficulty holding its body upright.

[c] ND, not described.

[d]Shivering.

pathway enzymes such as Gb_3 synthase, a glycosyltransferase, add the terminal galactose to complete Gb_3, other glycosyltransferases in the pathway are unique in each step of glycolipid synthesis, and there are catabolic pathway enzymes as well (see Fig. 6). All these enzymes participate in determining the amount of Gb_3 in the cell. Measuring these Gb_3-associated enzymes may provide more insight into Stx receptor regulation.

Discussion about How Stx Enters CNS of Animals

Purified Stx peripheral injection (intraperitoneal [i.p.] or intravenous [i.v.]) is able to induce CNS impairment similar to that of STEC oral infection, suggesting that there is a direct effect of Stx on CNS parenchymal cells. The rat model of intraventricular purified Stx2 injection in which purified Stx2 is inoculated directly into CNS

TABLE 3 Shiga toxin and/or LPS administration model with CNS descriptions

Ref.	Animal[a]	Toxin	CNS[b]	Gb_3/Stx binding	Histopathology[c,d,e]	Imaging	IHC[f]	Injection route[g]	Other assays
66	Baboon[h]	Stx1	ND	ND	EM: mye deg, peri ede, large neu and glia deg, cap normal	ND	ND	i.v.	
67	Baboon	Stx1	Yes	ND	ND	ND	ND	i.v.	
39	Weaned YL pigs	Stx2e	Yes	ND	Gross: Sc ede, CL ede and hrrgHE: CL hrrg but not ede or cap nec, no lesions in CR, BS, thalamus	ND	ND	i.v.	
40	Weaned YL pigs	Sup[i] Stx2e	Yes	ND	HE: CL, sub ede, hrrg, cap necHE: MB, fib nec , peri eos	ND	ND	i.v.	
41	NZW rabbit	Stx1	Yes	TLC-Stx1 over lay of CL, BS and Sc (+) at $LacCer^{j}$ position	HE: BS, Sc, CL cap narrowed, peri ede, cap damage and fib, Purkinje decreased	ND	ND	i.v.	
42	NZW rabbit	Stx1	Yes	^{125}I-Stx1 tissue distribution high in cecum, brain, small intestine, colon, Sc	HE: cerv Sc hrrg, inf, ede, fib in cap, lum Sc fib cap, pyk cap	ND	Anti-Stx (+) in Sc cap	i.v.	
52	JW rabbit	Stx2	Yes	ND	EM: mye deg, axo normal	MRI: V3 (24 h), later BS, cc, lateral amy, CL vermis	Immuno EM-DAB[k]: anti-Stx2 (+) at luminal side of cap, deg mye	i.v.	Tracer
47	JW rabbit	Stx2	Yes	ND	CR ctx, CL ctx, Sc, pyk neu, str neu not affected, inf in MB and CL	ND	Anti-Stx2 IHC (+) cap and sub	i.v. and i.t.	Stx2 ↑ in CSF
65	JW rabbit	Stx2	ND	ND	ND	MRI: CL at 82 h	ND	i.v.	Stx2 ↑ in CSF
65	JW rabbit	Stx2	ND	ND	ND	MRI: the rear of CL (contact w CSF) at 48 h	ND	i.t.	ND
68	JW rabbit	Stx2	Yes	ND	ND	MRI: BS and cerv Sc dorsal close to death	ND	i.v.	Baroreflex function
69	JW rabbit	Stx1	ND	ND	ND	MRI: MB, BS and Sc ede, cerv Sc dorsal hematoma	ND	i.v.	Stx1 ↑ slightly in CSF
54	JW rabbit young	Stx2	Yes	ND	HE: inf CL, myo thickening, fib, pyk and fragmented, pons myo nec	ND	Anti-Stx2 IHC(+) in pons cap and myo, anti-ssDNA IHC small number cap (+), IHC caspase-3 and-9 small number (+)	i.v.	
43	JW rabbit	Stx2	Yes	Anti-Gb_3 (+) in cap lum Sc	HE: inf lum Sc with hrrg and fib cap, str neu pyk, hippos pyr neu apop	ND	TUNEL + in hippo (DG, CA1, CR ctx neu, pons glia, capIHC: Ib4↑ (microglia activated) in lum Sc and thalamus	i.v.	qRT-PCR: TNFα↑ and IFNβ ↑
70	JW rabbit	Stx2	ND	ND	ND	MRI: Gd leak (↑permeability)	ND	i.v.	

48	DB rabbit	Stx2	Yes	ND	HE: neu deg in the BS	ND	ND	i.v.	
49	SD rat	Stx2	ND	ND	ND	ND	Anti-Stx IHC (+) peri	i.p.	
49	SD rat	Stx2	ND	ND	EM: irregular shape neu, mye deg, hypertrophic axo, astro phago mye, neu apop, deg, vacuol, peri astro ede, non-peri astro gliosis, oligo pathologic	ND	Anti-Stx2 (+) in neu, immune-EM-DAB: anti-Stx2 (+) in neu fibers and astro nucleus	i.c.v.	
58	SD rat	Stx2	ND	ND	ND	ND	Stx2 (+) in anterior hippo astro, ips hippo Stx2 (+) astro and neu, cont hippo Stx2(+) neuropils	i.c.v.	Str and CR ctx neu↓, cap↓ NADPH-d/NOS activity
57	SD rat	Stx2	Yes	Anti-Gb_3↑ CA1, str neu	ND	ND	Anti-Stx2↑ MAP2 ↑ CA1 neu.Anti-bax ↑neu (inner ctx, CA1, subV dorsal str, hypothalamic peri	i.c.v.	
50	SD rat	Sup Stx2	ND	ND	Nissle: neu pyk hypertrophy axo, ede ctx, subV CL.	ND	Anti-AQP4↓ cp	i.p.	
35	ICR mouse	Stx2	Yes	ND	ND	ND	Immune-EM-DAB: anti-Stx2 (+) mye deg, lyso pyr ctx	i.p.	Tracer
44	C57BL/6 mouse	Stx2	Yes	ND	HE: pyk oligo astro nuclei, hrrg sub	ND	ND	i.v.	
44	C57BL/6 mouse	Stx2 + LPS	Yes	ND	HE: hrrg BS sub severe than Stx2 alone	ND	ND	i.v.	
45	ICR mouse	Stx2	ND	ND	HE: congestion CL and hippo,hrrg CL, neu and glia normal	ND	Anti-Stx2 IHC (+) in RBC and cap CL, MB and thalamus,anti-Stx2 IHC (−) in neu, glia	i.v.	
63	C57BL/6 a4galt$^{-/-}$	Stx1 and Stx2	Not susceptible to Stx1	Anti-Gb_3 became negative in cap	ND	ND	ND	Not specified	
53	C57BL/6 mouse	Stx2	Yes	Anti-Gb_3 (+) in neu mouse and human Sc, human cap	EM: glia lamellipodia-like foot process interrupts synapse at motor neu of lum Sc		Immuno-gold EM*l:* anti-Gb_3 and anti-Stx2 double positive in motor neu of lum Sc	i.p.	
51	NIH mouse	Stx2	ND	ND	EM: neu, astro and peri ede, synaptic disruption, oligo defect			i.v.	Behavioral motor test +
61	Human	NA	NA	DRG*m*, Stx1 binding (+) neu and cap	NA	NA	NA	NA	
61	Rabbit	NA	NA	DRG, Stx1 binding (+) neu and cap	NA	NA	NA	NA	
61	Rat	NA	NA	DRG, Stx1 binding (+) neu	NA	NA	NA	NA	
62	Human	NA	NA	DRG, anti-Gb_3 and Stx1 binding (+) neu and cap	NA	NA	NA	NA	

(continued)

TABLE 3 Shiga toxin and/or LPS administration model with CNS descriptions *(continued)*

Ref.	Animal[a]	Toxin	CNS[b]	Gb_3/Stx binding	Histopatholog[c,d,e]	Imaging	IHC[f]	Injection route[g]	Other assays
62	Rabbit	NA	NA	DRG, anti-Gb_3 and Stx1 binding (+) neu and cap	NA	NA	NA	NA	
62	Rat	NA	NA	DRG, anti-Gb_3 and Stx1 binding (+) neu	NA	NA	NA	NA	
62	Mouse	NA	NA	DRG, anti-Gb_3 and Stx1 binding (+) neu	NA	NA	NA	NA	
60	C57BL/6 mouse	NA	NA	Anti-Gb_3 (+) neu at olf, CR ctx, str, hippo, hypothalamus, CVOs, CL, MO, ScV3 ependyma	NA	NA	NA	NA	

[a]Animal keys: YL, Yorkshire-Landrace; NZW, New Zealand White; JW, Japanese White; DB, Dutch Belted; SD, Sprague-Dawley.

[b]Detailed CNS symptoms are summarized in Table 2. ND, not described; NA, not applicable.

[c]Histopathology analysis keys are Gross, gross observation in non-stained tissue; HE, hematoxylin-esosin stain that stains cytoplasm in pink and nucleus blue, light microscopic findings (LM); PAS, periodic acid-Schiff stain that detects polysaccharides, glycoproteins and glycolipid, LM; LFB, Luxol fast blue stain that stains myelin in blue, LM; EM, electron microscopic findings.

[d]CNS regions and cell type abbreviations are CR, cerebrum; ctx, cortex; hippo, hippocampus; DG, dentate gyrus; str, striatum and other basal ganglia; CL, cerebellum; MO, medulla oblongata; MB, midbrain; BS, brain stem is used where midbrain, pons, or medulla oblongata are not specified; Sc, spinal cord; cerv, cervical; tho, thoracic; lum, lumbaris; sub, subarachnoid space. Histopathologic feature abbreviations are cap, endothelial cells or capillaries; inf, infarction; hrrg, hemorrhage; fib, fibrin deposition; nec, necrosis; swl, swelling; peri, perivascular; myo, myocytes; apop, apoptotic; mono, monocytes; mye, myelin; deg, degeneration; pyk, pyknotic nuclei; prolif, proliferation/hyperplasia; ede, edema; pyr, pyramidal neuron; inflt, infiltration of blood cells to parenchyma; neu, neuron; Purkinje, Purkinje cells are large neurons in CL; V3, third ventricle; cc, corpus callosum; amy, amygdala; ips, ipsilateral, injection side of brain; cont, contlateral, opposite of injection side; subV, subventricular region; cp, choroid plexus; CVO, circumventricular organs.

[e]Histopathologic feature abbreviations are cap, endothelial cells or capillaries; inf, infarction; hrrg, hemorrhage; fib, fibrin deposition; nec, necrosis; swl, swelling; peri, perivascular; myo, myocytes; apop, apoptotic, mono, monocytes; mye, myelin;, degeneration; pyk, pyknotic nuclei; prolif, proliferation/hyperplasia; ede, edema; pyr, pyramidal neuron; inflt, infiltration of blood cells to parenchyma; neu, neuron; Purkinje, Purkinje cells are large neurons in CL; glia, glial cells such as astrocytes, microglia, and oligodendrocytes); eos, eosinophilic globules, deposits); axo, axon, axoplasm; astro, astrocyte; oligo, oligodendrocyte; phago, phagocytosis; lyso, lysosome; RBC, red blood cells.

[f]IHC, immunohistochemistry, immunodetection of the target in the tissue sections.

[g]Injection route abbreviations: i.v., intravenous; i.t. (intrathecal, injection from cysterna magna that makes it possible to inject into cerebrospinal fluid (CSF); i.p., intraperitoneal; i.c.v., intracerebroventricular injection that injects solution directly into CNS parenchyma of cerebral cortex/ventricle.

[h]Baboon in this chart is *Papio c. cynocephalus*, or *Papio c. Anubis*

[i]Sup, *E. coli* culture supernatant.

[j]LacCer, lactsylceramide; adding galastose to LacCer completes Gb_3.

[k] Immuno-EM-DAB: immunodetection of the target with 3,3'-diaminobenzidine deposition by electron microscopy.

[l] Immuno-gold EM: immunodetection of the target with 5- to-10-nm gold particle allows precise localization as well as double labeling.

[m] DRG, dorsal root ganglion, a peripheral nervous system structure consisting of sensory neurons and other cell types.

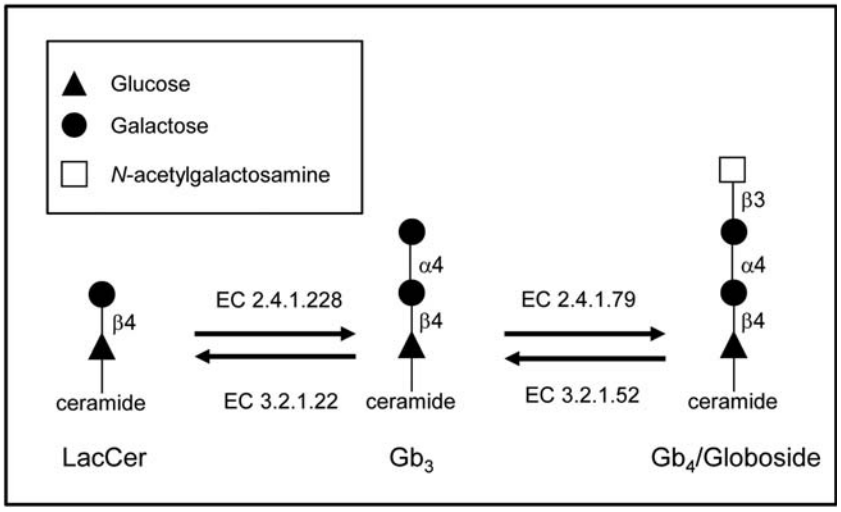

FIGURE 6 Metabolic and catabolic pathway enzymes for Gb_3 synthesis. A part of Gb_3 synthesis pathway is shown. From lactosylceramide (LacCer) to Gb_3, alpha 1, 4-galactosyltransferase (EC 2.4.1.228) adds a galactose to LacCer to produce Gb_3. Likewise, UDP-GalNAc: beta 1,3-galactosaminyltransferase (EC 2.4.1.79) works on Gb_3 to make Gb_4. In the catabolic pathway, beta-hexosaminidase (EC 3.2.1.52) degrades Gb_4 to Gb_3, and alpha-galactosidase (EC 3.2.1.22) makes LacCer from Gb_3. doi:10.1128/microbiolspec.EHEC-0005-2013.f6

parenchyma also induces similar CNS symptoms such as lethargy, hind-leg weakness, or paralysis (57). These results suggest that Stx released from STEC internalizes into the blood and then transfers to CNS parenchyma and asserts its toxicity.

The route and CNS region of Stx permeabilization are of great interest to explain which part of the CNS is most likely influenced by Stx. Stx injected by i.v. has been detected in cerebrospinal fluid (CSF) (rabbit [47, 65]). This suggests there is translocation of Stx from blood to CSF. A reduction of AQP1 in choroid plexus in rat with Stx (i.p.) suggests that there is weakening of the blood-CSF barrier in this location that may allow Stx to enter CSF from the blood. The ependymal cells lining at the third ventricle are a border between CSF and CNS parenchyma. Our group showed in mouse CNS that ependymal cells at the third ventricle are expressing Gb_3 in a naïve state (61). The tracer horseradish peroxidase that is injected intrathecally into CSF crossed and entered ependymal cells and parenchyma (rabbit [52]), and magnetic resonance imaging showed the third ventricle area with a bright signal that is an indication of leakiness into the fluid in this area. Taken together, it is reasonable to think that Stx uses blood-CSF barrier penetration as one of the routes into CNS parenchyma. On the other hand, Stx injected i.p. was detected in the perivascular area in rat (49), and BBB weakening was suggested by the reduction of AQP4 (rat [50], mouse [56], and by tracer horseradish peroxidase (i.v.) detection in parenchyma (mouse [35]). These results suggest that Stx can also use the BBB crossing route to enter the CNS. An important fact to note is that purified Stx by itself, without any other bacterial component, can enter CNS and assert its toxicity regardless of differences in receptor-expressing cell types among different species.

ACKNOWLEDGMENT

This work was supported by National Institutes of Health grants 5U01AI075778-05 and 1R56AI090144-01A1 to F.O.

REFERENCES

1. Ohmura M, Yamamoto M, Tomiyama-Miyaji C, Yuki Y, Takeda Y, Kiyono H. 2005. Nontoxic Shiga toxin derivatives from *Escherichia coli* possess adjuvant activity for the augmentation of antigen-specific immune responses via dendritic cell activation. *Infect Immun* **73:**4088–4097.

2. Tesh VL, Ramegowda B, Samuel JE. 1994. Purified Shiga-like toxins induce expression of proinflammatory cytokines from murine peritoneal macrophages. *Infect Immun* **62:**5085–5094.

3. Obrig TG. 2010. *Escherichia coli* Shiga toxin mechanisms of action in renal disease. *Toxins (Basel)* **2:**2769–2794.

4. Obrig TG, Karpman D. 2012. Shiga toxin pathogenesis: kidney complications and renal failure. *Curr Top Microbiol Immunol* **357:**105–136.

5. Karpman D, Sartz L, Johnson S. 2010. Pathophysiology of typical hemolytic uremic syndrome. *Semin Thromb Hemost* **36:**575–585.

6. Habib R, Mathieu H, Royer P. 1967. [Hemolytic-uremic syndrome of infancy: 27 clinical and anatomic observations]. *Nephron* **4:**139–172. (In French.)

7. Obrig TG, Louise CB, Lingwood CA, Boyd B, Barley-Maloney L, Daniel TO. 1993. Endothelial heterogeneity in Shiga toxin receptors and responses. *J Biol Chem* **268:**15484–15488.

8. Psotka MA, Obata F, Kolling GL, Gross LK, Saleem MA, Satchell SC, Mathieson PW, Obrig TG. 2009. Shiga toxin 2 targets the murine renal collecting duct epithelium. *Infect Immun* **77:**959–969.

9. Simon M, Cleary TG, Hernandez JD, Abboud HE. 1998. Shiga toxin 1 elicits diverse biologic responses in mesangial cells. *Kidney Int* **54:**1117–1127.

10. Shibolet O, Shina A, Rosen S, Cleary TG, Brezis M, Ashkenazi S. 1997. Shiga toxin induces medullary tubular injury in isolated perfused rat kidneys. *FEMS Immunol Med Microbiol* **18:**55–60.

11. Hughes AK, Stricklett PK, Kohan DE. 1998. Cytotoxic effect of Shiga toxin-1 on human proximal tubule cells. *Kidney Int* **54:**426–437.

12. Ghosh SA, Polanowska-Grabowska RK, Fujii J, Obrig T, Gear AR. 2004. Shiga toxin binds to activated platelets. *J Thromb Haemost* **2:**499–506.

13. Karpman D, Manea M, Vaziri-Sani F, Stahl AL, Kristoffersson AC. 2006. Platelet activation in hemolytic uremic syndrome. *Semin Thromb Hemost* **32:**128–145.

14. Fernandez GC, Rubel C, Dran G, Gomez S, Isturiz MA, Palermo MS. 2000 Shiga toxin-2 induces neutrophilia and neutrophil activation in a murine model of hemolytic uremic syndrome. *Clin Immunol* **95:**227–234.

15. Roche JK, Keepers TR, Gross LK, Seaner RM, Obrig TG. 2007. CXCL1/KC and CXCL2/MIP-2 are critical effectors and potential targets for therapy of *Escherichia coli* O157:H7-associated renal inflammation. *Am J Pathol* **170:**526–537.

16. Foster GH, Armstrong CS, Sakiri R, Tesh VL. 2000. Shiga toxin-induced tumor necrosis factor alpha expression: requirement for toxin enzymatic activity and monocyte protein kinase C and protein tyrosine kinases. *Infect Immun* **68:**5183–5189.

17. Eaton KA, Friedman DI, Francis GJ, Tyler JS, Young VB, Haeger J, Abu-Ali G, Whittam TS. 2008. Pathogenesis of renal disease due to enterohemorrhagic *Escherichia coli* in germ-free mice. *Infect Immun* **76:**3054–3063.

18. Stahl AL, Sartz L, Nelsson A, Bekassy ZD, Karpman D. 2009. Shiga toxin and lipopolysaccharide induce platelet-leukocyte aggregates and tissue factor release, a thrombotic mechanism in hemolytic uremic syndrome. *PLoS One* **4:**e6990.

19. Keepers TR, Psotka MA, Gross LK, Obrig TG. 2006. A murine model of HUS: Shiga toxin with lipopolysaccharide mimics the renal damage and physiologic response of human disease. *J Am Soc Nephrol* **17:**3400–3414.

20. Keepers TR, Gross LK, Obrig TG. 2007 Monocyte chemoattractant protein 1, macrophage inflammatory protein 1 alpha, and RANTES recruit macrophages to the kidney in a mouse model of hemolytic-uremic syndrome. *Infect Immun* **75:**1229–1236.

21. Hasko G, Linden J, Cronstein B, Pacher P. 2008. Adenosine receptors: therapeutic aspects for inflammatory and immune diseases. *Nat Rev Drug Discov* **7:**759–770.

22. Walters MD, Matthei IU, Kay R, Dillon MJ, Barratt TM. 1989. The polymorphonuclear leucocyte count in childhood haemolytic uraemic syndrome. *Pediatr Nephrol* **3:**130–134.

23. Inward CD, Howie AJ, Fitzpatrick MM, Rafaat F, Milford DV, Taylor CM. 1997. Renal histopathology in fatal cases of diarrhoea-associated haemolytic uraemic syndrome. *Pediatr Nephrol* **11:**556–559.

24. Griener TP, Strecker JG, Humphries RM, Mulvey GL, Fuentealba C, Hancock RE, Armstrong GD. 2011. Lipopolysaccharide renders transgenic mice expressing human serum amyloid P component sensitive to Shiga toxin 2. *PLoS One* **6:**e21457.

25. Kawachi H, Han GD, Miyauchi N, Hashimoto T, Suzuki K, Shimizu F. 2009. Therapeutic targets in the podocyte: findings in anti-slit diaphragm antibody-induced nephropathy. *J Nephrol* **22:**450–456.

26. Das L, Brunner HI. 2009. Biomarkers for renal disease in childhood. *Curr Rheumatol Rep* **11:**218–225.

27. Trachtman H, Christen E, Cnaan A, Patrick J, Mai V, Mishra J, Jain A, Bullington N, Devarajan P. 2006 Urinary neutrophil gelatinase-associated lipocalcin in D+HUS: a novel marker of renal injury. *Pediatr Nephrol* **21:**989–994.

28. Mohawk KL, O'Brien AD. 2011. Mouse models of *Escherichia coli* O157:H7 infection and Shiga toxin injection. *J Biomed Biotechnol* **2011:**258185.

29. Karpman D, Connell H, Svensson M, Scheutz F, Alm P, Svanborg C. 1997. The role of lipopolysaccharide and Shiga-like toxin in a mouse model of *Escherichia coli* O157:H7 infection. *J Infect Dis* **175:**611–620.

30. Wadolkowski EA, Sung LM, Burris JA, Samuel JE, O'Brien AD. 1990. Acute renal tubular necrosis and death of mice orally infected with *Escherichia coli* strains that produce Shiga-like toxin type II. *Infect Immun* **58:**3959–3965.

31. Tzipori S, Chow CW, Powell HR. 1988. Cerebral infection with *Escherichia coli* O157:H7 in humans and gnotobiotic piglets. *J Clin Pathol* **41:**1099–1103.

32. Dean-Nystrom EA, Pohlenz JF, Moon HW, O'Brien AD. 2000. *Escherichia coli* O157:H7 causes more-severe systemic disease in suckling piglets than in colostrum-deprived neonatal piglets. *Infect Immun* **68:**2356–2358.

33. Matise I, Sirinarumitr T, Bosworth BT, Moon HW. 2000. Vascular ultrastructure and DNA fragmentation in swine infected with Shiga toxin-producing *Escherichia coli*. *Vet Pathol* **37:**318–327.

34. Shringi S, Garcia A, Lahmers KK, Potter KA, Muthupalani S, Swennes AG, Hovde CJ, Call DR, Fox JG, Besser TE. 2012. Differential virulence of clinical and bovine-biased enterohemorrhagic *Escherichia coli* O157:H7 genotypes in piglet and Dutch belted rabbit models. *Infect Immun* **80:**369–380.

35. Fujii J, Kita T, Yoshida S, Takeda T, Kobayashi H, Tanaka N, Ohsato K, Mizuguchi Y. 1994. Direct evidence of neuron impairment by oral infection with verotoxin-producing *Escherichia coli* O157:H- in mitomycin-treated mice. *Infect Immun* **62:**3447–3453.

36. Kurioka T, Yunou Y, Kita E. 1998. Enhancement of susceptibility to Shiga toxin-producing *Escherichia coli* O157:H7 by protein calorie malnutrition in mice. *Infect Immun* **66:**1726–1734.

37. Isogai E, Isogai H, Kimura K, Hayashi S, Kubota T, Fujii N, Takeshi K. 1998. Role of tumor necrosis factor alpha in gnotobiotic mice infected with an *Escherichia coli* O157:H7 strain. *Infect Immun* **66:**197–202.

38. Taguchi H, Takahashi M, Yamaguchi H, Osaki T, Komatsu A, Fujioka Y, Kamiya S. 2002. Experimental infection of germ-free mice with hyper-toxigenic enterohaemorrhagic *Escherichia coli* O157:H7, strain 6. *J Med Microbiol* **51:**336–343.

39. MacLeod DL, Gyles CL, Wilcock BP. 1991. Reproduction of edema disease of swine with purified Shiga-like toxin-II variant. *Vet Pathol* **28:**66–73.

40. Gannon VP, Gyles CL, Wilcock BP. 1989. Effects of *Escherichia coli* Shiga-like toxins (verotoxins) in pigs. *Can J Vet Re*. **53:**306–312.

41. Zoja C, Corna D, Farina C, Sacchi G, Lingwood C, Doyle MP, Padhye VV, Abbate M, Remuzzi G. 1992. Verotoxin glycolipid receptors determine the localization of microangiopathic process in rabbits given verotoxin-1. *J Lab Clin Med* **120:**229–238.

42. Richardson SE, Rotman TA, Jay V, Smith CR, Becker LE, Petric M, Olivieri NF, Karmali MA. 1992. Experimental verocytotoxemia in rabbits. *Infect Immun* **60:**4154–4167.

43. Takahashi K, Funata N, Ikuta F, Sato S. 2008. Neuronal apoptosis and inflammatory responses in the central nervous system of a rabbit treated with Shiga toxin-2. *J Neuroinflammation* **5:**11.

44. Sugatani J, Igarashi T, Munakata M, Komiyama Y, Takahashi H, Komiyama N, Maeda T, Takeda T, Miwa M. 2000. Activation of coagulation in C57BL/6 mice given verotoxin 2 (VT2) and the effect of co-administration of LPS with VT2. *Thromb Res* **100:**61–72.

45. Nishikawa K, Matsuoka K, Kita E, Okabe N, Mizuguchi M, Hino K, Miyazawa S, Yamasaki C, Aoki J, Takashima S, Yamakawa Y, Nishijima M, Terunuma D, Kuzuhara H, Natori Y. 2002. A therapeutic agent

with oriented carbohydrates for treatment of infections by Shiga toxin-producing *Escherichia coli* O157:H7. *Proc Natl Acad Sci USA* **99:**7669–7674.

46. Taylor CM, Williams JM, Lote CJ, Howie AJ, Thewles A, Wood JA, Milford DV, Raafat F, Chant I, Rose PE. 1999. A laboratory model of toxin-induced hemolytic uremic syndrome. *Kidney Int* **55:**1367–1374.

47. Mizuguchi M, Tanaka S, Fujii I, Tanizawa H, Suzuki Y, Igarashi T, Yamanaka T, Takeda T, Miwa M. 1996. Neuronal and vascular pathology produced by verocytotoxin 2 in the rabbit central nervous system. *Acta Neuropathol (Berl)* **91:**254–262.

48. Garcia A, Marini RP, Catalfamo JL, Knox KA, Schauer DB, Rogers AB, Fox JG. 2008. Intravenous Shiga toxin 2 promotes enteritis and renal injury characterized by polymorphonuclear leukocyte infiltration and thrombosis in Dutch Belted rabbits. *Microbes Infect* **10:**650–656.

49. Goldstein J, Loidl CF, Creydt VP, Boccoli J, Ibarra C. 2007. Intracerebroventricular administration of Shiga toxin type 2 induces striatal neuronal death and glial alterations: an ultrastructural study. *Brain Res* **1161:**106–115.

50. Lucero MS, Mirarchi F, Goldstein J, Silberstein C. 2012. Intraperitoneal administration of Shiga toxin 2 induced neuronal alterations and reduced the expression levels of aquaporin 1 and aquaporin 4 in rat brain. *Microb Pathog* **53:**87–94.

51. Tironi-Farinati C, Geoghegan PA, Cangelosi A, Pinto A, Loidl CF, Goldstein J. 2013. A translational murine model of sub-lethal intoxication with Shiga toxin 2 reveals novel ultrastructural findings in the brain striatum. *PLoS One* **8:**e55812.

52. Fujii J, Kinoshita Y, Kita T, Higure A, Takeda T, Tanaka N, Yoshida S. 1996. Magnetic resonance imaging and histopathological study of brain lesions in rabbits given intravenous verotoxin 2. *Infect Immun* **64:**5053–5060.

53. Obata F, Tohyama K, Bonev AD, Kolling GL, Keepers TR, Gross LK, Nelson MT, Sato S, Obrig TG. 2008. Shiga toxin 2 affects the central nervous system through receptor globotriaosylceramide localized to neurons. *J Infect Dis* **198:**1398–1406.

54. Mizuguchi M, Sugatani J, Maeda T, Momoi T, Arima K, Takashima S, Takeda T, Miwa M. 2001. Cerebrovascular damage in young rabbits after intravenous administration of Shiga toxin 2. *Acta Neuropathol (Berl)* **102:**306–312.

55. Kita E, Yunou Y, Kurioka T, Harada H, Yoshikawa S, Mikasa K, Higashi N. 2000. Pathogenic mechanism of mouse brain damage caused by oral infection with Shiga toxin-producing *Escherichia coli* O157:H7. *Infect Immun* **68:**1207–1214.

56. Amran MY, Fujii J, Suzuki SO, Kolling GL, Villanueva SY, Kainuma M, Kobayashi H, Kameyama H, Yoshida S. 2013. Investigation of encephalopathy caused by Shiga toxin 2c-producing *Escherichia coli* infection in mice. *PLoS One* **8:**e58959.

57. Tironi-Farinati C, Loidl CF, Boccoli J, Parma Y, Fernandez-Miyakawa ME, Goldstein J. 2010. Intracerebroventricular Shiga toxin 2 increases the expression of its receptor globotriaosylceramide and causes dendritic abnormalities. *J Neuroimmunol* **222:**48–61.

58. Meuth SG, Gobel K, Kanyshkova T, Ehling P, Ritter MA, Schwindt W, Bielaszewska M, Lebiedz P, Coulon P, Herrmann AM, Storck W, Kohmann D, Muthing J, Pavenstadt H, Kuhlmann T, Karch H, Peters G, Budde T, Wiendl H, Pape HC. 2013. Thalamic involvement in patients with neurologic impairment due to Shiga toxin 2. *Ann Neurol* **73:**419–429.

59. Boccoli J, Loidl CF, Lopez-Costa JJ, Creydt VP, Ibarra C, Goldstein J. 2008. Intracerebroventricular administration of Shiga toxin type 2 altered the expression levels of neuronal nitric oxide synthase and glial fibrillary acidic protein in rat brains. *Brain Res* **1230:**320–333.

60. Winter KR, Stoffregen WC, Dean-Nystrom EA. 2004. Shiga toxin binding to isolated porcine tissues and peripheral blood leukocytes. *Infect Immun* **72:**6680–6684.

61. Obata F, Obrig T. 2010 Distribution of Gb(3) immunoreactivity in the mouse central nervous system. *Toxins (Basel)* **2:**1997–2006.

62. Ren J, Utsunomiya I, Taguchi K, Ariga T, Tai T, Ihara Y, Miyatake T. 1999. Localization of verotoxin receptors in nervous system. *Brain Res* **825:**183–188.

63. Utsunomiya I, Ren J, Taguchi K, Ariga T, Tai T, Ihara Y, Miyatake T. 2001. Immunohistochemical detection of verotoxin receptors in nervous system. *Brain Res Brain Res Protoc* **8:**99–103.

64. Okuda T, Tokuda N, Numata S, Ito M, Ohta M, Kawamura K, Wiels J, Urano T, Tajima O, Furukawa K. 2006. Targeted disruption of Gb3/CD77 synthase gene resulted in the complete deletion of globo-series glycosphingolipids and loss of sensitivity to verotoxins. *J Biol Chem* **281:**10230–10235.

65. Fujii J, Kinoshita Y, Yamada Y, Yutsudo T, Kita T, Takeda T, Yoshida S. 1998. Neurotoxicity of intrathecal Shiga toxin 2 and protection by intrathecal injection of anti-Shiga toxin 2 antiserum in rabbits. *Microb Pathog* **25:**139–146.

66. Taylor CM, Williams JM, Lote CJ, Howie AJ, Thewles A, Wood JA, Milford DV, Raafat F, Chant I, Rose PE. 1999. A laboratory model of toxin-induced hemolytic uremic syndrome. *Kidney Int* **55:**1367–1374.

67. Siegler RL, Pysher TJ, Lou R, Tesh VL, Taylor FB, Jr. 2001. Response to Shiga toxin-1, with and without lipopolysaccharide, in a primate model of hemolytic uremic syndrome. *Am J Nephrol* **21:**420–425.

68. Yamada Y, Fujii J, Murasato Y, Nakamura T, Hayashida Y, Kinoshita Y, Yutsudo T, Matsumoto T, Yoshida S. 1999. Brainstem mechanisms of autonomic dysfunction in encephalopathy-associated Shiga toxin 2 intoxication. *Ann Neurol* **45:**716–723.

69. Fujii J, Kinoshita Y, Yutsudo T, Taniguchi H, Obrig T, Yoshida SI. 2001. Toxicity of Shiga toxin 1 in the central nervous system of rabbits. *Infect Immun* **69:**6545–6548.

70. Fujii J, Kinoshita Y, Matsukawa A, Villanueva SY, Yutsudo T, Yoshida S. 2009. Successful steroid pulse therapy for brain lesion caused by Shiga toxin 2 in rabbits. *Microb Pathog* **46:**179–184.

71. Tzipori S, Gunzer F, Donnenberg MS, de Montigny L, Kaper JB, Donohue-Rolfe A. 1995. The role of the eaeA gene in diarrhea and neurological complications in a gnotobiotic piglet model of enterohemorrhagic *Escherichia coli* infection. *Infect Immun* **63:**3621–3627.